Flow boiling heat transfer of a non-azeotropic mixture inside a single microchannel

Davide DEL COL *, Marco AZZOLIN, Stefano BORTOLIN

* Corresponding author: Tel.: +39 049 8276891; Fax: +39 049 8276896; Email: davide.delcol@unipd.it
Department of Industrial Engineering, University of Padova, IT

Abstract This study moves from the need to study flow boiling of zeotropic mixture in microchannels. In the recent years much attention has been paid to the possible use of fluorinated propene isomers for the substitution of high-GWP refrigerants. The available HFOs (hydrofluoroolefins) cannot cover all the air-conditioning, heat pump, and refrigeration systems when used as pure fluids because their thermodynamic properties are not suitable for all operating conditions and therefore some solutions may be found using blends of refrigerants, to satisfy the demand for a wide range of working conditions. In the present paper a mixture of R1234ze(E) and R32 (0.5/0.5 by mass) has been studied. The local heat transfer coefficient during flow boiling of this mixture in a single microchannel with 0.96 mm diameter is measured at a pressure of 14 bar, which corresponds to a bubble temperature of 26.3°C. The flow boiling data taken in the present test section are discussed, with particular regard to the effect of heat flux, mass velocity and vapor quality. The heat transfer coefficients are compared against some predicting models available in the literature. Furthermore, the new experimental data are compared to flow boiling data of pure R1234ze(E) and pure R32 to analyze the heat transfer penalization due to the mass transfer resistance of this zeotropic mixture.

Keywords: Microchannels, Flow Boiling, Non-azeotropic mixture, Heat transfer

1. Introduction

A significant and still growing part of the engineering research community has been devoted in the last few decades to scaling down devices, while keeping or even increasing their functionality. Furthermore, recent technical applications in the electronic industry demand high heat flux dissipation from small areas. The introduction of microchannels in the field of enhanced heat transfer and in the refrigeration and air conditioning sectors is surely one attempt to respond to these needs. Microchannels allow to develop compact elements which work with reduced refrigerant charge minimizing the problems of release of potentially hazardous fluids in the atmosphere and can usually withstand extremely high system pressures.

The need for achieving high heat transfer rates in compact heat exchangers goes along with the request of suitable refrigerants possessing low global warming potential (GWP). The reason for much of this interest can be attributed to the growing number of regulations and laws at international level. In 2012, the European Commission proposed to cut F-gas emissions by two-thirds by 2030. The search for alternatives primarily focuses on the use of natural refrigerants (hydrocarbons, ammonia, carbon dioxide) and new synthetic refrigerants having low GWP. Halogenated olefins (HFOs) have been investigated as refrigerants and those with fluorinated propene isomers as R1234yf and R1234ze(E) have emerged as possible solutions. Even if they are already commercialized, the HFOs cannot cover all the air-conditioning, heat pump, and refrigeration systems because of their thermodynamic properties. In recent studies, it was found that the coefficient of performance (COP) and the capacity of heat pump cycles using R1234ze(E) are significantly lower than those of the most widely used refrigerant, R410A (Koyama et al. 2010). The causes are related to the properties of R1234ze(E) which are reported in Table 1.

Fluid	p_{sat} [bar]	ρ_l [kg m^{-3}]	ρ_v [kg m^{-3}]	μ_l [μPa s]	μ_v [μPa s]	λ_l [W m^{-1} K^{-1}]	h_{lv} [kJ kg^{-1}]
R32	24.783	893.0	73.3	94.99	13.83	0.115	237.09
R134a	10.166	1146.7	50.1	161.45	12.37	0.075	163.02
R1234ze(E)	7.666	1111.3	40.7	167.00	12.93	0.069	154.80

Tab.1: Refrigerant properties at 40°C.

To improve the COP and, in the latest literature it was attempted to blend R1234ze(E) with R32. Although R32 is a HFCs, it has relatively lower GWP and excellent thermodynamic characteristics. As the result of their drop-in test with R32/R1234ze(E) 0.5/0.5 by mass, Koyama et al. (2010) concluded that the tested binary mixture achieved a superior COP at some operating conditions, and proposed this binary mixture is the most promising candidate to replace R410A. Regarding the vaporization of the mixture R32/R1234ze(E), Kondou et al. (2013) performed flow boiling tests in a horizontal microfin tube of 5.21 mm inner diameter at different mass compositions. The heat transfer coefficient and pressure drop are measured at a saturation temperature of 10°C, heat fluxes of 10 and 15 kW m^{-2}, and mass velocities from 150 to 400 kg m^{-2} s^{-1}. Hossain et al. (2013) measured the heat transfer coefficient of the mixture at 45/55% mass composition (R32/R1234ze(E)) inside a 4.35 mm tube. So far this mixture has not been studied in microchannels. Furthermore, very limited data are available in the literature regarding flow boiling of zeotropic mixtures in microchannels.

In this work, a mixture of R1234ze(E) and R32 (0.5/0.5 by mass) is studied during flow boiling in a single microchannel with 0.96 mm diameter at 14 bar saturation pressure, corresponding to a bubble temperature of 26.3°C. As a peculiar characteristic of the present work, the heat transfer coefficient is not measured by imposing the heat flux; instead, the boiling process is governed by controlling the inlet temperature of the heating secondary fluid. On this regard the present data is new and original since the large majority of data in the literature is taken by means of Joule effect heating.

2. Experimental apparatus

The test rig used for the experimental tests consists of the primary (refrigerant) loop and of two auxiliary loops: the hot water loop to promote boiling and the cold water loop to control the refrigerant condensation after the test section. In the primary loop, the subcooled refrigerant from the condenser is sent into an independently controlled gear pump, which is magnetically coupled to a variable speed electric motor. The fluid is then pumped through the Coriolis-effect mass flow meter into the test section as a subcooled liquid. The refrigerant enters the test section, which is made of two counter-flow heat exchangers. The first one (pre-conditioning sector) is used to achieve the desired inlet condition and the second one is the actual measuring sector. The pressure is gauged through two digital pressure (absolute and differential) transducers, connected to manometric taps to measure the fluid pressure upstream and downstream of the test tube. The water flow rate in the pre-conditioning sector and in the measuring sector, is measured by means of two Coriolis-effect mass flow meters and the total temperature difference of water across both sectors is measured with two copper-constantan thermopiles.

The test section is obtained from a thick wall copper drawn tube for industrial applications, with 0.96 mm inside diameter. The mean roughness *Ra*, as defined by the ISO 4287 (1997), has been measured and ranges between 0.98 μm and 1.61 μm, with a mean value of 1.30 μm. The thermocouples embedded in the wall are installed in 0.6 mm diameter cylindrical holes, machined 0.5 mm away from the internal tube surface. The measuring sector is 228 mm long and is equipped with 15 thermocouples in the water and 11 in the wall. A detailed description of the experimental apparatus is reported in Del Col et al. (2013a).

3. Data reduction

In the present setup, the heat flux is determined from the temperature profile of the coolant in the measuring sector. The water temperature is experimentally measured in 15 positions in the coolant path. The wall temperature is measured by means of thermocouples embedded in the copper tube. Since the wall thermocouples are installed 0.5 mm far from the internal tube surface, a correction is required for the wall temperature measurement due to the distance between the thermocouple and the inner tube surface.

Fig. 1 shows the refrigerant, wall and water temperature profile along the measuring sector during flow boiling of R32/R1234ze(E) mixture at G=400 kg m^{-2} s^{-1}. The refrigerant enters the test channel at 22.7°C, with 3.6 K subcooling. At the exit, the refrigerant temperature is increased by 5.4 K from the bubble temperature (26.3°C at 14 bar) because evaporation of a two components mixture is a non-isothermal process and during boiling the refrigerant temperature evolves towards the dew temperature. The water enters from the opposite side of the test tube at 38.5°C and its temperature decreases due to the heat transfer to the boiling refrigerant. As it can be seen, the refrigerant and the water temperature profiles match well (the refrigerant-to-water temperature difference is pretty constant, 6.3 K) leading to a reduction of the exergy losses associated with the heat transfer.

A limited number of publications reported data of thermophysical properties for the mixture R32/R1234ze(E). Among them Akasaka (2013) presents thermodynamic property models for this mixture: it emphasizes that the models proposed are designed not for scientific use but for engineering use and they are based on limited experimental data. For the R32/R1234ze(E) the KW2 model with tuned parameters better fits the experimental data and it is here implemented in REFPROP (Lemmon et al., 2013) to determine the mixture properties.

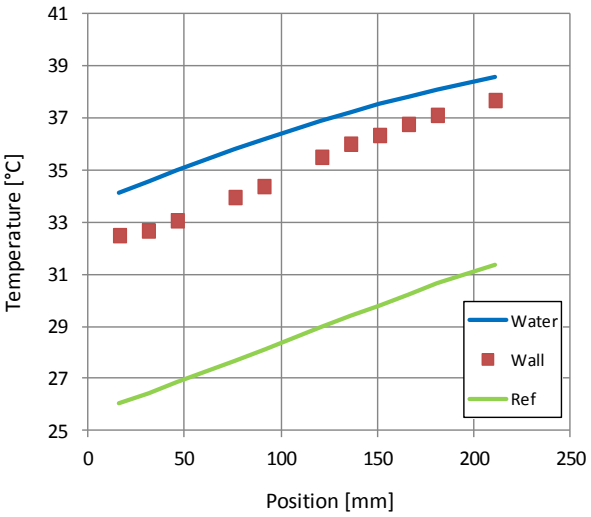

Fig. 1. Water, wall and refrigerant temperature during vaporization of R32/R1234ze(E) mixture at 400 kg m^{-2} s^{-1}.

3.1 Heat flux

Since the heat flux is not directly fixed here, it must be obtained indirectly, from the slope of the secondary fluid temperature profile:

$$q' = \dot{m}_w \cdot c_{p,w} \cdot \frac{1}{\pi d} \frac{\mathrm{d}T_w}{\mathrm{d}z} \qquad (1)$$

where z is the axial coordinate along the tube and $\mathrm{d}T_w/\mathrm{d}z$ is the derivative of the water temperature along z. In the calculation, a polynomial function is used to interpolate the water temperature profile along the channel. Two different independent procedures have been adopted for the determination of the fitting polynomial degree of the water temperature and thus the calculation of the heat flux (Eq. 1). The first criterion, dubbed as physical, is based on the assumption that all the calculated values by the polynomial interpolation of the water temperatures should be below ±0.05 K with respect to the experimental values. Beside this, a statistical method based on the choice of the simplest fitting polynomial has been used. This statistic approach uses the R^2 statistic parameter, and adjusts it on the basis of the residual degrees of freedom: this is the reason of the name R^2_{adj} (Rawlings et al. 1998).

3.2 Heat transfer coefficient and vapor quality

The local heat transfer coefficient α_i inside the microchannel is obtained as the ratio of heat flux to temperature difference:

$$\alpha_i = \frac{q_i'}{\left(T_{wall,i} - T_{ref,i}\right)} \tag{2}$$

where the wall temperature is directly measured by the thermocouples embedded in the wall. The refrigerant temperature at the *i-th* thermocouple location, assuming an equilibrium state, is calculated from the pressure, enthalpy and mixture composition as proposed in Kondou et al. (2013):

$$T_{ref,i} = f\left(p_i, h_i, X_{R1234ze}\right) \tag{3}$$

The vapor quality *x* at any axial position *z*, similarly to the refrigerant temperature, is calculated from the pressure, enthalpy and mixture composition.

The refrigerant enthalpy at the position of the *i-th* wall thermocouple is obtained from a heat balance between the mixture and the water that flows in counter-flow:

$$h_{ref,i} = h_{sub} + \frac{\dot{m}_w}{\dot{m}_{ref}} c_{p,w}\left(T_{w,out} - T_{w,i}\right) \tag{4}$$

The enthalpy of the subcooled refrigerant is determined from the inlet pressure and temperature.

Since the refrigerant pressure is measured at inlet and outlet of the test section, a linear variation is usually assumed in the channel. However, during vaporization, the vapor quality changes along the microchannel and therefore the pressure gradient varies in the measuring sector; for this reason, a linear interpolation of the saturation pressure between inlet and outlet may lead to errors in the determination of the heat transfer coefficient. In the present work the pressure profile along the microchannel is calculated by implementing the Del Col et al. (2013b) two-phase pressure gradient correlation. The calculated pressure gradient is then corrected by an empirical coefficient to match the experimental total pressure drop to the value measured by the differential pressure transducer. Once the pressure profile is known, the local refrigerant temperature can be determined from the enthalpy at each channel location.

4. Flow boiling results

Flow boiling tests have been performed with the mixture R32/R1234ze(E) at 0.5/0.5 by mass composition, at mass velocity ranging between 300 and 600 kg m^{-2} s^{-1}, at a pressure of 14 bar , in a 0.96 mm round microchannel. The refrigerant enters the test section as saturated liquid and the vapor quality change in the test section varies from 20% to 80%.

During the test runs only mass velocities and inlet fluid temperatures can be fixed; thus the heat flux varies along the process and this complicates the comparison of the present tests to the ones obtained with electrical heating.

4.1 Degradation of the heat transfer coefficient

Fig. 2 reports the heat transfer coefficient of the mixture and the pure fluids at about 100 kW m^{-2} and G = 400 kg m^{-2} s^{-1}. The refrigerant mixture displays lower heat transfer coefficients than those of the single pure fluids. The heat transfer degradation from an ideal behavior is about 50% at *x* equal to 0.4. Similar results displaying, heat transfer coefficients of the mixture R32/R1234ze(E) lower than either of the single components, are reported in Kondou et al. (2013).

This degradation is mostly caused by the bubble point temperature increase at the bubble interface or at the liquid-vapor interface due to the mole fraction gradient at the interface, created by the volatility difference of the two pure components. During the evaporation process the liquid becomes richer in R1234ze(E) (less volatile component) and the vapor becomes richer of R32 (the more volatile). The heat transfer coefficient reduction is caused by the diffusion of the more volatile component to the interface and the concentration of the less volatile

component at the heated surface is not favorable to bubble nucleation. Beside this, a part of the heat transfer coefficient reduction is due to the added heat flow rate needed to heat liquid and vapor to the boiling temperature, constantly increasing along the tube.

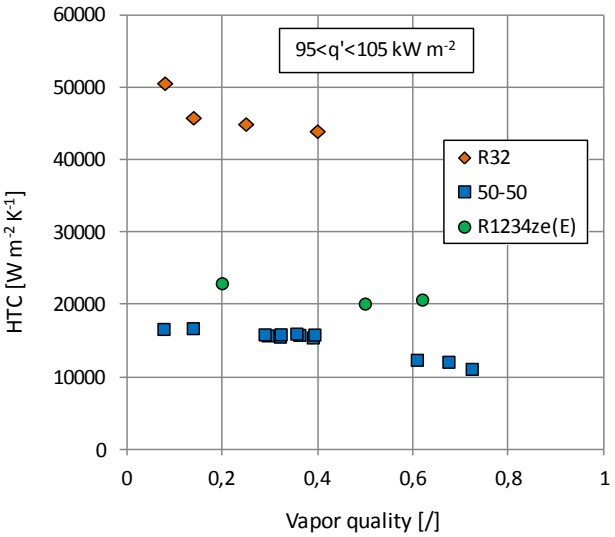

Fig. 2. Local heat transfer coefficient for pure R32, pure R1234ze(E) and the mixture R32/R1234ze(E) at G = 400 kg m^{-2} s^{-1}.

4.2 Effect of heat flux

As previously mentioned, in this work the heat flux is not electrically imposed: the controlled parameters are the inlet fluid temperatures and the mass flow rate of the secondary fluid. As a consequence, for each test run, not only the heat transfer coefficient and the vapor quality vary along the channel but also the heat flux is a variable. Therefore, with the present technique, it is impossible to get the heat transfer coefficient variation with vapor quality at fixed heat flux as reported in literature using electric heating. In order to explore the effects of heat flux and vapor quality on the heat transfer coefficient, several tests were made at constant refrigerant mass velocity and varying the inlet water conditions (mass flux and temperature). A further data processing is then required to investigate the effects of vapor quality, mass velocity and heat flux on the heat transfer coefficient.

The effect of heat flux on the heat transfer coefficient can be better understood in Fig. 3 where the heat transfer coefficient has been reported at constant mass velocity and limited vapor quality range around 0.2.

At a constant vapor quality, the heat transfer coefficient increases with heat flux. The present heat transfer coefficients are dependent on heat flux even if at the higher heat flux the heat transfer coefficient seems to become less dependent on the heat flux and tend to constant values.

4.3 Effect of vapor quality and mass velocity

By processing data at constant heat flux, it is possible to get information on the effect of vapor quality. Fig. 4 shows the experimental trend of heat transfer coefficient for the mixture R32/R1234ze(E) at different mass velocities and vapor quality, for a heat flux of about 100 kW m^{-2}.

For the pure refrigerant components, in the same test section, Del Col et al. (2013a, 2013c) found that the heat transfer coefficients were highly dependent on the heat flux, increased with heat flux in the saturated region and the mass flux had no effect. They reported also a decreasing of the heat transfer coefficient with vapor quality at constant heat flux.

Similarly to the results for the pure refrigerant components (Del Col et al. 2013a, 2013c) the heat transfer coefficient of the refrigerant mixture decreases with vapor quality for all the mass velocity at around 100 kW m^{-2} (Fig. 4).

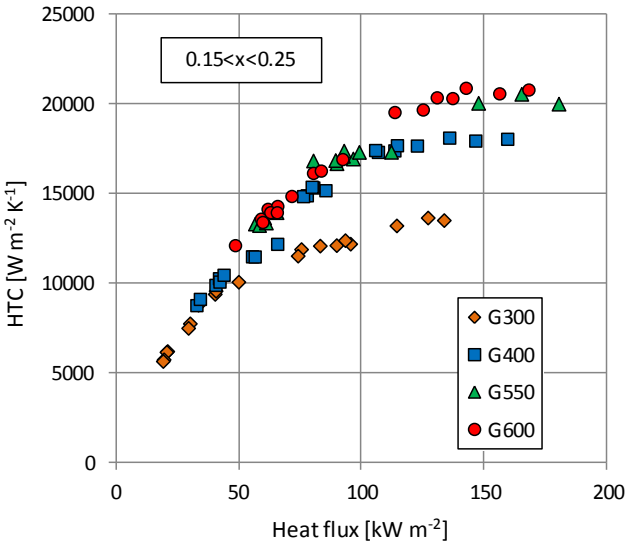

Fig. 3. Local heat transfer coefficient versus heat flux at constant vapor quality for the 50/50% R32/R1234ze(E) mixture.

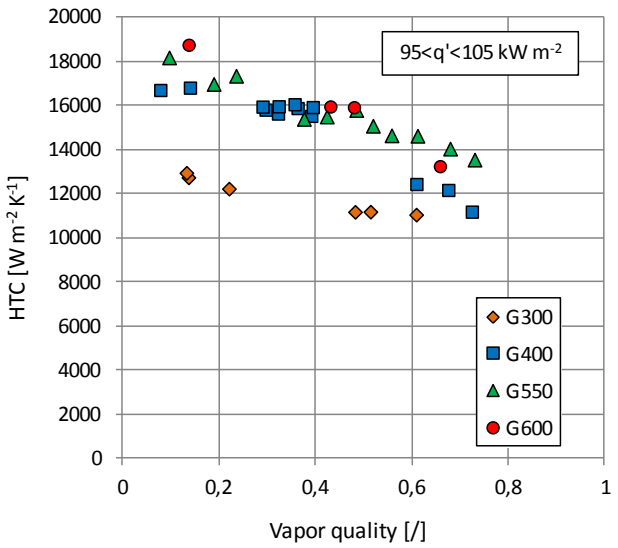

Fig. 4. Local heat transfer coefficient versus vapor quality during vaporization at constant heat flux for the 50/50% R32/R1234ze(E) mixture.

In Fig. 3 and Fig. 4 a mass velocity effect is shown. The heat transfer coefficient increases with the mass velocity at the higher heat flux. From the data it seems that the effect of the additional mass transfer resistance is reduced by increasing the mass velocity.

5. Comparison against models.

During vaporization of a zeotropic mixture an adequate model or correction to account for the additional mass transfer resistance must be considered. Hereafter the correlations by Gungor and Winterton (1986) and Sun and Mishima (2009) have been corrected as follows.

To take into account the sensible heating of the vapor phase, as reported by Cavallini et al. (1998), the heat transfer coefficient of the mixture is:

$$\alpha_m = \left(\frac{1}{\alpha_f} + \frac{\partial q_{sg} / \partial q_t}{\alpha_g} \right)^{-1} \qquad (5)$$

where α_f is the heat transfer coefficient pertinent to the liquid film, α_g is the convective heat transfer coefficient of the vapor phase, $\partial q_{sg}/\partial q_t$ is the ratio between the sensible heat flow rate heating the vapor and the total heat flow rate. The term $(\partial q_{sg}/\partial q_t)/\alpha_g$ is analogous to the one obtained by Bell and Ghaly (1973) for condensation of zeotropic mixture. If the ratio of dT/dh remains approximately constant during the vaporization process the term in Eq. (5) can be rewritten as:

$$\frac{\partial q_{sg}}{\partial q_t} \approx x c_{pg} \frac{\Delta T_{GL}}{\Delta h_m} \qquad (6)$$

where Δh_m is the isobaric change in enthalpy of the mixture at given composition.

The heat transfer coefficient in the liquid film α_f can be calculated with an appropriate flow boiling correlation utilizing the physical properties of the mixture correcting the nucleate boiling component for mass diffusion effect as suggested by Thome (1996). The correction factor F_c (Eq. 7) was analytically developed by Thome (1989).

$$F_c = \left[1 + \left(\frac{\alpha_{fb,id}\ \Delta T_{GL}}{q'} \right) \left(1 - e^{-\left(\frac{Bq'}{\rho_l \Delta h_m \beta_l} \right)} \right) \right] \qquad (7)$$

The heat flux to be used in Eq. (7) is the local nucleate boiling heat flux but; as a first approximation, the total heat flux can be used.

In the Gungor and Winterton (1986) correlation the correction factor was applied to the nucleate boiling contribution

$$\alpha_{gw} = \alpha_{nb}\ F_c + \alpha_{cv} \qquad (8)$$

In the correlation of Sun and Mishima (2009) F_c was applied as reported in Eq. (9)

$$\alpha_{sm} = \frac{6\,\mathrm{Re}_{lo}^{1.05} \left(Bo \cdot F_c \right)^{0.54}}{We_l^{0.191} \left(\frac{\rho_l}{\rho_g} \right)^{0.142}} \frac{\lambda_l}{d} \qquad (9)$$

In the database considered in the following comparison the heat flux ranges between 20 and 180 kW m^{-2} and the vapor quality between 0.1 and 0.8. Only data points characterized by vaporization prior to onset of dryout are considered.

The comparison with the model of

Gungor and Winterton (1986) corrected as in Eq. (8) is shown in Fig. 5. On average, this model seems to be able to predict well the experimental trend and slightly overestimates the data. Higher deviations are observed at low heat flow rate.

In Fig. 6, the present experimental data are compared with predicted heat transfer coefficient values by Sun and Mishima (2009) model corrected for a zeotropic mixture. This correlation is based upon the Lazarek and Black (1982) model and takes the effect of Weber number into account. An improvement in the prediction of heat transfer coefficients for pure fluids with respect to the Lazarek and Black (1982) model has been found by Del Col et al. (2013a, 2013c). Considering the present mixture data, the Sun and Mishima (2009) corrected correlation is able to predict the data for almost all the data points within the ±30% error band.

6. Conclusions

In the present work the authors report the measurements of the local flow boiling coefficient of a zeotropic mixture in a 0.96 mm diameter single circular microchannel, using a secondary fluid instead of fixing the heat flux by electric heating. The heat transfer coefficient at around 14 bar saturation pressure is measured for a R1234ze(E)/R32 mixture at 0.5/0.5 mass composition.

The experimental heat transfer coefficient decreases with vapor quality for all the tested mass velocities; it is dependent on the heat flux although it tends to a constant value at the higher heat flux.

When the heat transfer coefficients of the refrigerant mixture are compared with those of the pure fluid components, it can be seen that the experimental values are lower than those from the ideal mixing law due to the additional mass transfer resistance. From the experimental data it seems that the effect of the additional mass transfer resistance is reduced increasing the mass velocity.

The present data have been compared against some predicting correlations available in the literature. The Gungor and Winterton (1986) and the Sun and Mishima (2009) correlations have been considered. The correlations have been corrected to take into account the effect of the mass transfer resistance and the sensible heating of the vapor phase. On average, these correlations corrected for zeotropic mixtures predict almost all the data in the ±30% error band.

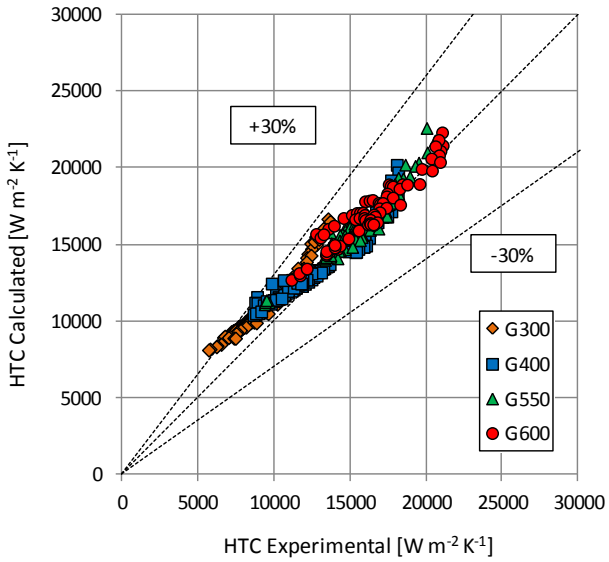

Fig. 5. Experimental data compared against the model by Gungor and Winterton (1986) corrected for a zeotropic mixture.

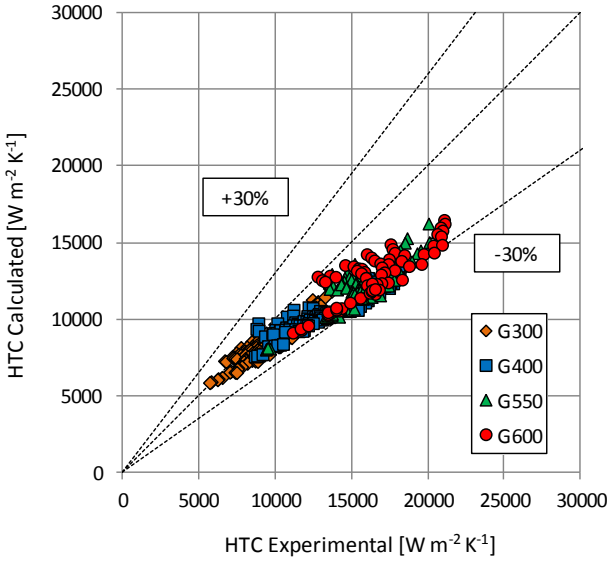

Fig. 6. Mixture R32/R1234ze(E) experimental data compared against model by Sun and Mishima (2009) corrected for zeotropic mixture.

Nomenclature

B	scaling factor assumed to be 1
Bo	Boiling number (-)
c_p	specific heat (J kg^{-1} K^{-1})

d hydraulic diameter (m)
F_c mixture correction factor (-)
G mass velocity (kg m^{-2} s^{-1})
h specific enthalpy (J kg^{-1})
HTC heat transfer coefficient (W m^{-2} K^{-1})
$\dot{m}$ mass flow rate (kg s^{-1})
p pressure (Pa)
q' heat flux (W m^{-2})
Ra arithmetical mean deviation of the profile according to ISO 4297:1997 (µm)
T temperature (K)
Re Reynolds number (-)
We Weber number (-)
x thermodynamic vapor quality (-)
X mass fraction (-)
z axial position

Greek symbols

α heat transfer coefficient (W m^{-2} K^{-1})
α_f HTC of the liquid film (W m^{-2} K^{-1})
α_g HTC of the vapor phase (W m^{-2} K^{-1})
$\alpha_{fb,id}$ ideal HTC calculated with pure refrigerant correlations (W m^{-2} K^{-1})
β_l = 0.0003 (m s^{-1}) liquid-phase mass transfer coefficient
ΔT temperature difference (K)
λ thermal conductivity (W $m^{-1}K^{-1}$)
ρ density (kg m^{-3})

Subscripts

cv convective boiling
fb flow boiling
g vapor
gv Gungor-Winterton
GL glide
i-th i-th thermocouple position
id ideal
in inlet
l liquid
m mixture
nb nucleate boiling
out outlet
ref refrigerant
s sensible
sm Sun-Mishima
sub subcooling
t total
w water

References

Akasaka, R., 2013. Thermodynamic property models for the difluoromethane (R-32) + trans-1,3,3,3-tetrafluoropropene (R-1234ze(E)) and difluoromethane + 2,3,3,3-tetrafluoropropene (R-1234yf) mixtures, Fluid Phase Eq. 358, 98-104.

Bell, K.J., Ghaly, M.A., 1973. An approximate generalized design method for multicomponent / partial condenser, AICHE Symp. Ser. 69, 72-79.

Cavallini, A., Del Col, D., Longo, G.A., Rossetto, L., 1998. Refrigerant vaporization inside enhanced tubes: a heat transfer model. Proc. Heat transfer in condensation and evaporation: Eurotherm seminar, Grenoble, France, 222-231.

Del Col, D., Bortolin, S., Rossetto, L., 2013a. Convective boiling inside a single circular microchannel, Int. J. Heat Mass Transfer 67, 1231-1245.

Del Col, D., Bisetto, A., Bortolato, M., Torresin, D., Rossetto, L., 2013b. Experiments and updated model for two phase frictional pressure drop inside minichannels, Int.J.Heat Mass Tran. 67(13),326–337.

Del Col, D., Bortolato, M., Bortolin, S., 2013c. Measurements of the heat transfer coefficient during flow boiling of two HFOs inside a circular microchannel. Proc. 8th World Conference on Experimental Heat Transfer, Fluid Mechanics, and Thermodynamics, Lisbon.

Gungor, K.E., Winterton, R.H., 1986. A general correlation for flow boiling in tubes and annuli, Int. J. Heat Mass Transfer 29, 351-358.

Hossain, Md. A., Onaka, Y., Afroz, H.M.M., Miyara, A., 2013. Heat transfer during evaporation of R1234ze(E), R32, R410A and a mixture of R1234ze(E) and R32 inside a horizontal smooth tube, Int. J. of Refrigeration 36, 465-477.

Kondou, C., BaBa, D., Mishima, F., Koyama, S., 2013. Flow boiling of non-azeotropic mixture R32/R1234ze(E) in horizontal microfin tubes, Int. J. of Refrigeration 36, 2366-2378.

Koyama, S., Takata, N., Fukuda, S., 2010. Drop-in experiments on heat pump cycle using HFO-1234ze(E) and its mixtures with HFC-32. Proc. Int. Refrigeration and Air Conditioning Conf. at Purdue, West Lafayette, IN, No. 2514, pp. 1e8.

Lazarek, G.M., Black, S.H., 1982. Evaporative heat transfer, pressure drop and critical heat flux in small vertical tube with R-113, Int. J. Heat Mass Transfer 25 (7), 945–960.

Lemmon, E.W., Huber, M.L., McLinden, M.O, 2013. NIST Standard Reference Database 23: Reference Fluid Thermodynamic and Transport Properties-REFPROP, Version 9.1, National Institute of Standards and Technology, Standard Reference Data Program, Gaithersburg.

Rawlings, J.O., Pantula, S.G., Dickey, D.A., 1998. Applied Regression Analysis, Springer, New York.

Sun, L., Mishima, K., 2009. An evaluation of prediction methods for saturated flow boiling heat transfer in mini-channels, Int. J. Heat Mass Transfer 52, 5323–5329.

Thome, J.R., 1989. Prediction of the mixture effect on boiling in vertical thermosyphon reboilers, Heat Transfer Eng. 10 (2), 29-38.

Thome, J.R., 1996. Boiling of new refrigerants: a state of the art review, Int. J. Refrig. 19(7),435-457.